

A Study of Soil Wave Propagation

R. K. BERNHARD, *Professor of Engineering Mechanics, Rutgers University, New Brunswick, N. J.*

• THIS REPORT discusses wave propagation in stratified sandy clays excited by sinusoidal force vectors of constant amplitudes. By adapting impact methods to this type of excitation certain soil characteristics may be determined. To check the results, reflection, refraction, and dispersion effects, as well as decay coefficients and strata depths, were computed. Their analysis yielded results which coincided reasonably well with values obtained from field experiments.

PREVIOUS INVESTIGATIONS

Impact Force Excitation

The classical theories developed by Rayleigh (1), Lamb (2), and Love (3) form the backbone of a well-established science in seismology. They show the co-existence of numerous types of propagating waves in the soil — such as longitudinal, shear, Rayleigh, Love, and hydrodynamic waves — each having different propagation velocities as well as trajectories (4-25).

Sinusoidal Force Excitation

The recent development of mechanical oscillators (16) generating sinusoidal force vectors permitted the application of discrete parameters such as magnitude, direction, frequency, and action line of the disturbing source. Hence, the uncertainty inherent in blasting methods with respect to these four parameters, as well as the resultant transients, could be eliminated.

PRESENT INVESTIGATION

From the foregoing limited citations of the pertinent literature it may be con-

cluded that any theoretical as well as experimental approach to the problems in soil dynamics is rather complex and certain simplifying assumptions cannot be avoided.

The purpose of the present study is as follows:

1. To compare some of the previous investigations.
2. To determine what simplifying assumptions are permissible.
3. To check whether the experimental results coincide with an analysis based on these assumptions.

One of the controversial suppositions is that two waves — one surface and one reflected or refracted body wave — may become predominant, which could be shown for restricted source detector distances. This rather provocative assumption of two waves of unknown characteristics facilitates the mathematical treatment substantially and should be considered as a temporary short cut only.

For an easily available check the factor of strata depth was selected. This depth could be determined analytically and verified by borings.

It must be emphasized that most of these studies are restricted to one specific case of stratified, non-compacted sandy clays.

Further investigations are required to determine whether similar results are obtainable under different conditions.

TECHNIQUE

Impact (blast) methods for geophysical prospecting — subsurface reconnaissance — to explore strata depth or oil sources are well known. The main difference between this approach and the

method described in the report is the manner of introducing propagating waves into the soil.

Excitation of propagating waves by earthquakes or blasts is replaced by adjustable sinusoidal force vectors of known magnitude, direction, and frequency. As far as could be established the earliest papers dealing with this method were published by the DEGEBO (10) and the author in 1936 (14). The use of sinusoidal force vectors with constant amplitudes instead of amplitudes increasing with the square of the frequency seems to be the first application of this particular type of excitation.

Instrumentation

The technique employed to induce sinusoidal propagating waves into the soil and to measure their effect by seismographs and pressure cells has been described elsewhere (15). A few relevant details inherent to this method might be mentioned.

The instrumentation comprised a mechanical three-mass oscillator (16) to excite sinusoidal force vectors of constant amplitude, seismometers to pick up the transmitted propagating waves on the soil surface, and pressure cells below the soil surface.

A sinusoidal vertical force vector ranging from about 500 lb to about 1,500 lb generated enough energy above the noise level (ground unrest) to be detectable at larger distances. The vertical components of the trajectory could be recorded up to 200 ft horizontally from the disturbance on the surface and pressure changes up to 60 ft horizontally below the surface.

The phase velocity is determined by the ratio of distance over time as traced simultaneously from the output of two transducers. The location of these two pick-ups yields the distance. The phase angle between two corresponding maxima of their records indicates the time. However, this phase velocity does not necessarily represent a true velocity, because reflection, refraction, and dispersion effects may be included.

Waves when excited by mechanical oscillators are of sinusoidal characteristics. They have the advantage of producing stationary patterns, which can be recorded continuously as soon as the exciter-soil system has reached a stable dynamic equilibrium (steady state).

The output of two adjacent transducers may be fed into a phase meter, a two-gun cathode-ray oscillograph, or *via* an electronic switch into a single-ray oscillograph. By synchronizing the wave frequency with the time signal (X-axis) of an oscillograph, two standing waves will appear on the screen (Fig. 1). The distance between corresponding maxima or minima, calibrated in feet per second, indicates the phase velocity directly. No time-consuming recording and additional calculations are necessary, as is usually the case when applying blast excitation.

The disadvantage of these continuous sinusoidal waves is that no characteristic wave fronts will be patterned. Hence, measurements at rather short distances between adjacent detectors are required to interpret correctly phase differences between two observation points. In other words, phase angles larger than 360° must be avoided.

Furthermore, wave type identification by means of first wave front arrivals is not possible.

Soils

The field available for investigation consisted mainly of four rather homogeneous strata (15). Figure 2 represents approximate depth profiles, including soil types, as obtained from three bore holes.

Layers A and B comprise a dry mixture of medium and coarse sandy clay. The upper bed, A, is a recent fill, the lower bed, B, an older stratum (11). Layer C, having the same composition, however, is located below the water table. Stratum D consists of hard clay. Layer E forms a lens of soft clay.

A few experiments were made on soil of similar composition as stratum A, with no detectable stratification to a depth of about 40 ft.

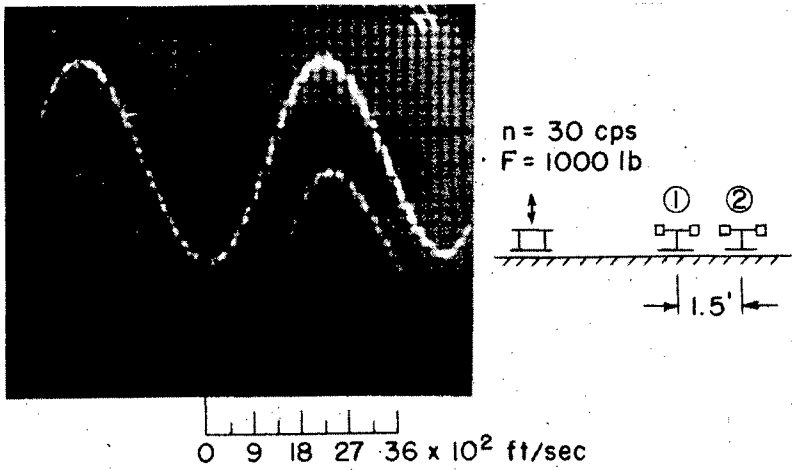


Figure 1. Seismometer records due to sinusoidal force excitation; stationary image on cathode-ray oscillograph screen; double pattern produced by electronic switch, $v_p = 450$ ft per sec.

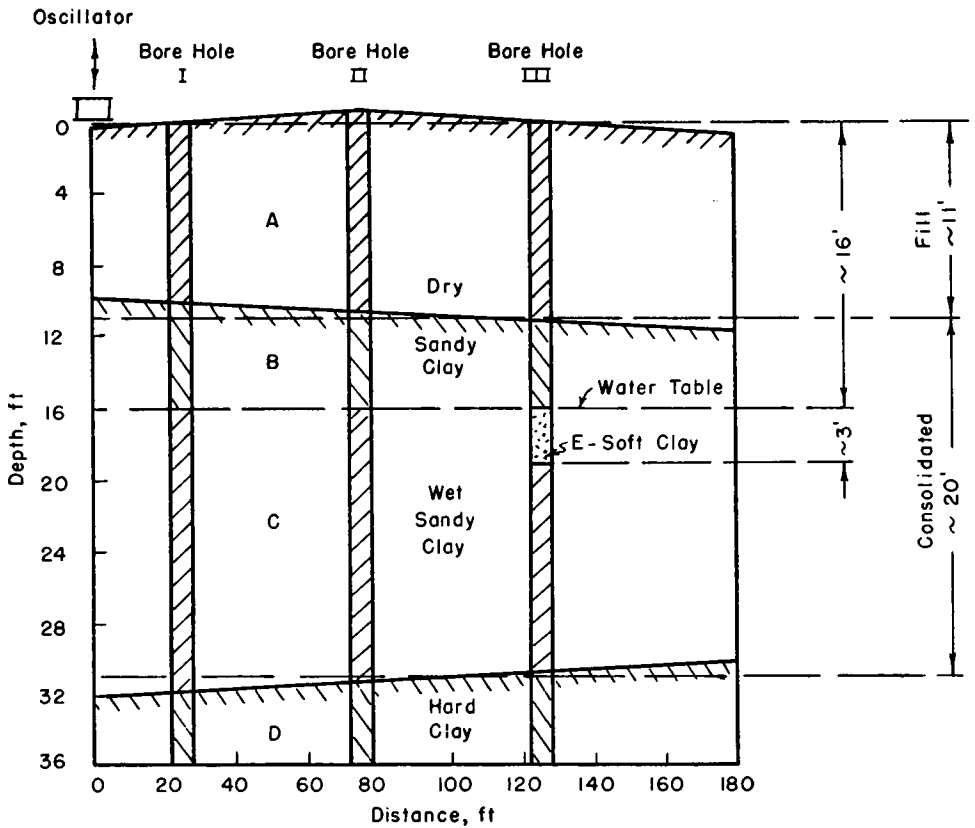


Figure 2. Depth profile obtained from borings.

Discussion

The advantages and disadvantages of sinusoidal force excitation when compared with blast methods are as follows:

Advantages:

1. Magnitude, direction, action line, and frequency of the sinusoidal force vector can be adjusted to and reproduced, as well as kept constant, for any desired values within the capacity range of the exciter.
2. Phase velocities may be read off directly from a stationary pattern.

Disadvantages:

1. The distance between two pick-up units must be smaller than the distance corresponding to one exciter period.
2. A mechanical oscillator, including drive and power supply, is heavier and more expensive than complete powder charge equipment.

Improvement of the instrumentation (in particular increased sensitivity of the transducer and recorder units) is planned for future tests.

Investigations on soils of different composition, stratification, water contents, etc., are essential.

VELOCITY OF PROPAGATING WAVES

The main purpose of this part of the investigation is a study on wave velocities due to impact and sinusoidal force excitation as obtained from seismograph and pressure-cell records. In the following discussion nine graphs have been selected as typical examples.

Components of Trajectory

Figure 3 is a record of three unidirectional seismographs all at a distance of 50 ft from the oscillator. Seismograph 1 indicates the transverse vertical (TV), seismograph 2 the transverse horizontal (TH), and seismograph 3 the longitu-

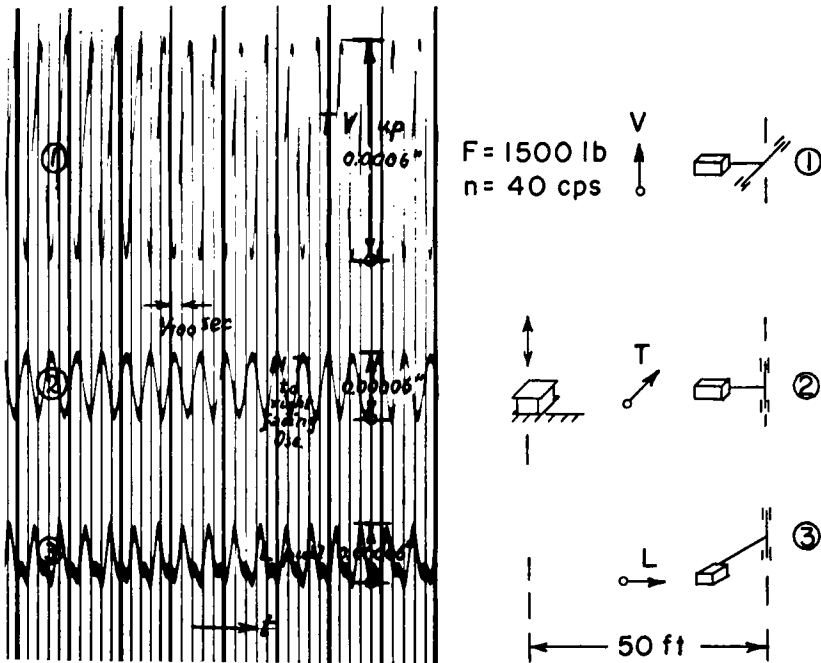


Figure 3. Seismograph records of components of trajectory due to sinusoidal force excitation, $d_1 = 50$ ft.

dinal horizontal (LH) component of the trajectory. Only the TV component is large enough to yield reliable results; the magnitudes of the TH and LH components are too small and partially masked by the noise level (ground unrest).

When comparing individual images of this as well as the following oscillographs, the difference in amplitudes due to the varying sensitivity of the transducers and amplifier units must be considered. In Figure 3 the TH and LH components required a much larger amplification than the TV component, as can be seen from the maximum displacements marked on the diagram. No orbits in space could be plotted from these records.

Hence, all further conclusions are based primarily on the TV components of the trajectory.

Velocity Determination

Impact Force Excitation. The first series of experiments was made on soil with no significant stratification to minimize reflection or refraction effects. Impacts could be produced by hammering a wooden stick into the ground. The lower end of this stick penetrated about 1 ft below the surface.

If Figure 4a represents the location of the disturbing force and of the detectors, and Figure 4b represents the corresponding displacement-time records, C and S, mark the arrivals of the first compression and shear wave fronts with the velocities v_c and v_s .

Then

$$v_c = \frac{d_{12}}{t_{12}} = \frac{d_{23}}{t_{23}} \quad (1)$$

$$\Delta t = t_s - t_c = \frac{d}{v_s} - \frac{d}{v_c} \quad (2)$$

or

$$v_s = \frac{d}{\Delta t + d/v_c} \quad (3)$$

and, finally,

$$\begin{aligned} v_s &= \frac{d_1}{\Delta t_1 + d_1/v_c} = \frac{d_2}{\Delta t_2 + d_2/v_c} \\ &= \frac{d_3}{\Delta t_3 + d_3/v_c} \quad (4) \end{aligned}$$

requiring the evaluation of only one wave train.

Figures 5 and 6 are seismograph records, Figures 7 and 8 are pressure cell records, due to impact excitation on non-stratified soil. The arrival of two wave fronts — first of the compression wave, C, and second of the shear wave, S — is visible. The arrival of the shear wave is not as clearly recognizable as would be the case with blast excitation.

An evaluation according to Eqs. 1 and 4 yielded $v_c \sim 1,100$ ft per sec and $v_s \sim 450$ ft per sec.

Sinusoidal Force Excitation. The second series of experiments was made on stratified sandy clay (Fig. 2) similar in composition to the soil used for impact tests as previously described.

If Figure 9a represents the location of the oscillator and the three detectors (1, 2, 3), and Figure 9b represents the recorded time-displacement diagrams, t_{12} and t_{23} are the time lags between the maxima of two adjacent transducers at the distances d_{12} and d_{23} , respectively. The assumption is made that d_{12} and d_{23} are smaller than the wave length, λ . Thus, the apparent phase velocity becomes

$$v_p = \frac{d_{12}}{t_{12}} = \frac{d_{23}}{t_{23}} \quad (5)$$

requiring the recording of two wave trains.

Figures 10 and 11 are seismograph records, Figures 12 and 13 are pressure cell records, due to sinusoidal excitation on stratified soil. The sinusoidal pattern and the time lag between the records (maxima or minima) of two adjacent detectors is clearly visible. The evaluation according to Eq. 5 yielded the apparent phase velocities. For a source-detector distance ranging from 50 to 69 ft, the apparent phase velocity was ~ 350 ft per sec at 20, 30, and 40 cps. All previously discussed velocity measurements are summarized in Table 1.

Discussion

1. The similarity of corresponding records of the TV-trajectory components,

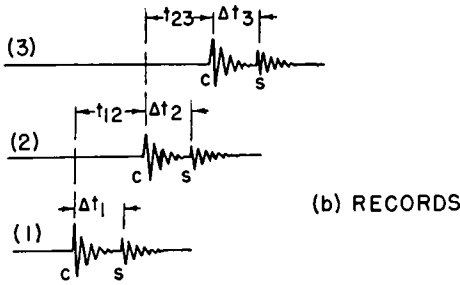
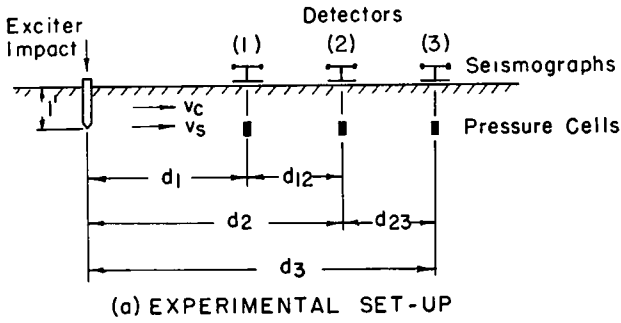
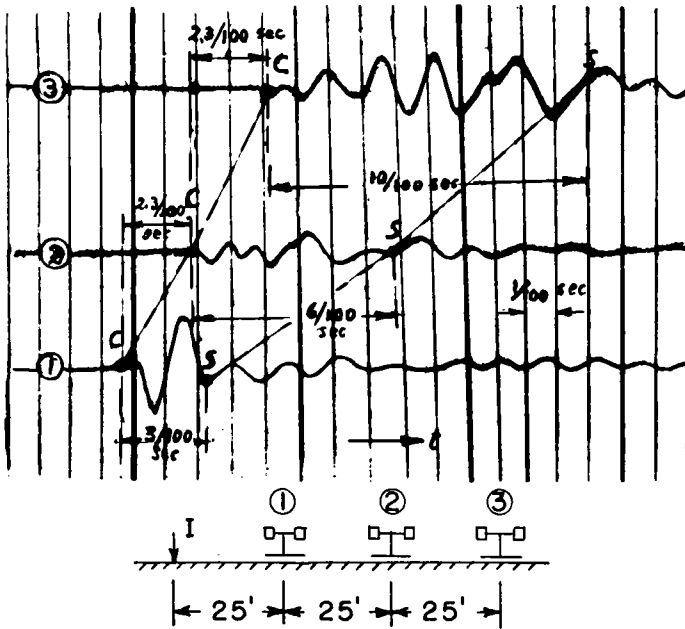


Figure 4. Phase velocity determination due to impact excitation.



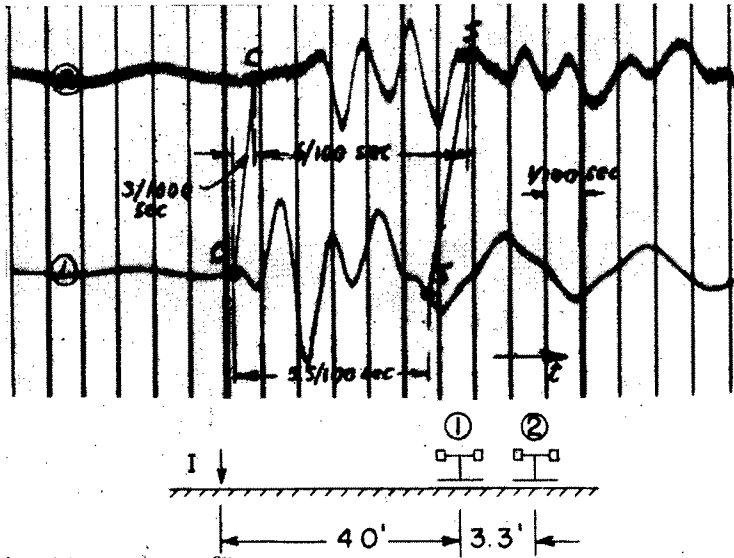


Figure 6. Seismograph records due to impact force excitation, $d_1 = 40$ ft: $v_c \sim 1,100$ ft/sec, $v_s \sim 440$ ft/sec.

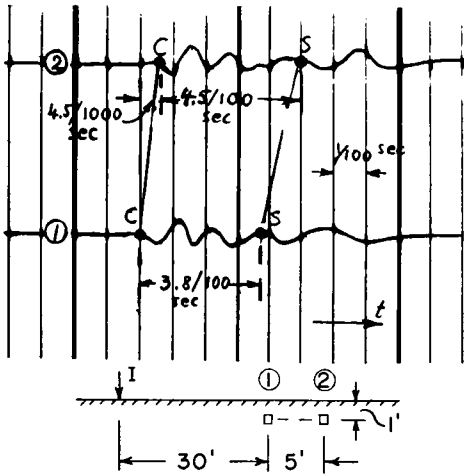


Figure 7. Pressure cell records due to impact force excitation, $d_1 = 30$ ft: $v_c \sim 1,100$ ft/sec, $v_s \sim 450$ ft/sec.

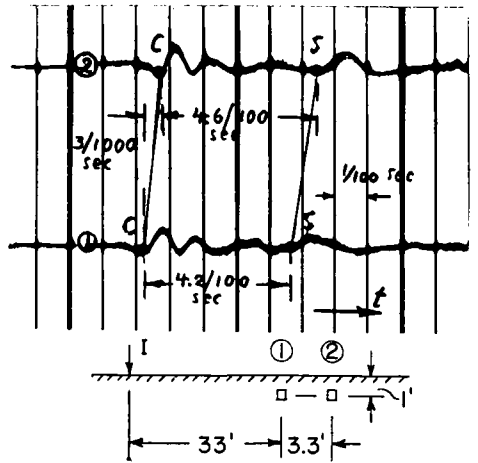


Figure 8. Pressure cell records due to impact force excitation, $d_1 = 33$ ft: $v_c \sim 1,100$ ft/sec, $v_s \sim 460$ ft/sec.

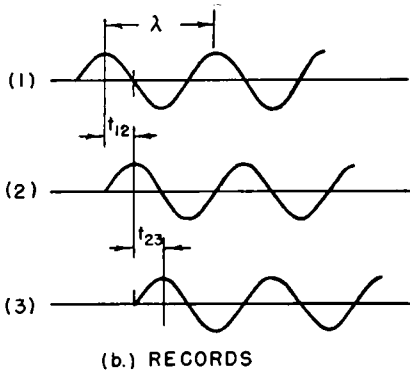
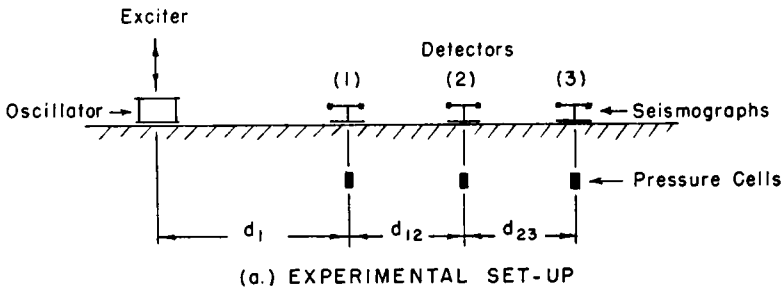


Figure 9. Phase velocity determination due to sinusoidal force excitation.

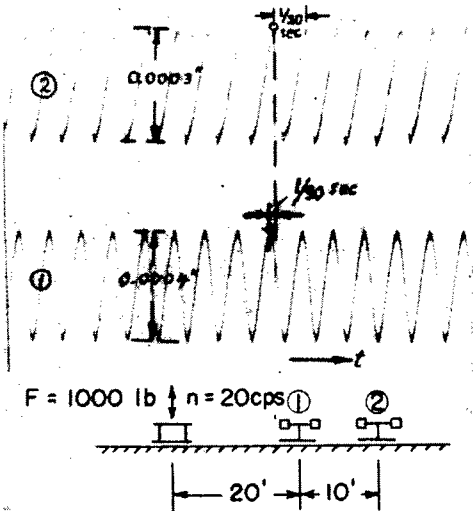


Figure 10. Seismograph records due to sinusoidal force excitation, $d_1 = 20 \text{ ft}$; $v_p \sim 900 \text{ ft/sec}$.

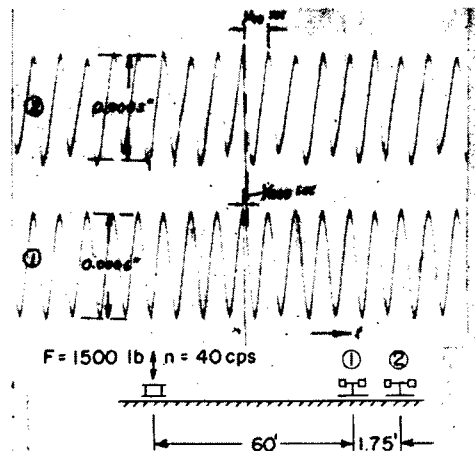


Figure 11. Seismograph records due to sinusoidal force excitation, $d_1 = 60 \text{ ft}$; $v_p \sim 450 \text{ ft/sec}$.

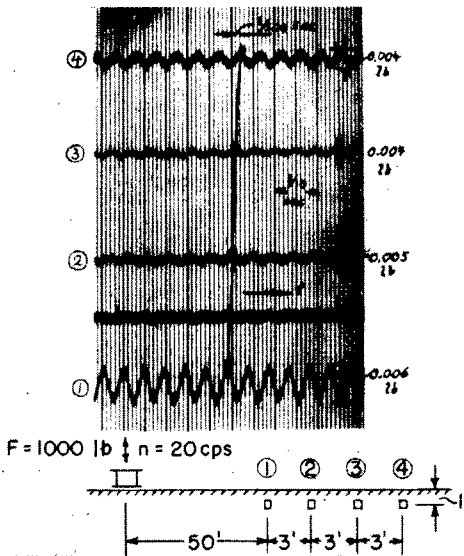


Figure 12. Pressure cell records due to sinusoidal force excitation, $d_1 = 50$ ft: $v_p \sim 300$ ft/sec.

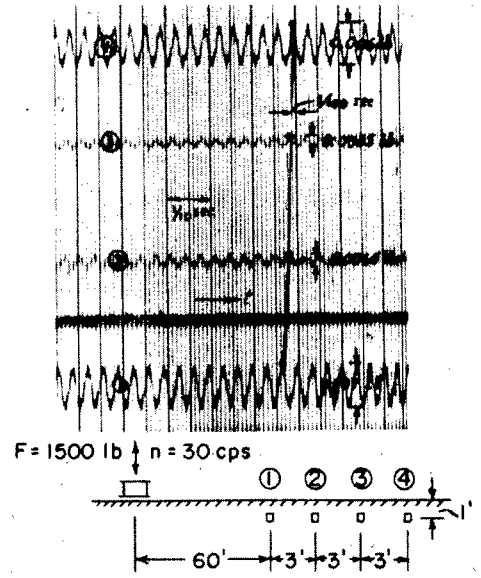


Figure 13. Pressure cell records due to sinusoidal excitation, $d_1 = 50$ ft: $v_p \sim 300$ ft/sec.

regardless of the various types of transmitters used, seems to indicate that the instrumentation operated satisfactorily. This reproducibility of all details is particularly striking for the transient phenomena recorded from impact excitation.

2. The velocities obtained from surface and subsurface measurements induced by impact excitation on non-stratified sandy clays averaged 450 ft per sec for the shear waves and 1,100 ft per sec for the compression waves. These two veloc-

ity values are used for the computations under "Type of Propagating Waves."

3. The apparent phase velocities gained from surface and subsurface measurements induced by sinusoidal force excitation on stratified sandy clays were in the range of 300 to 900 ft per sec. Velocities of similar magnitude are introduced in the computations under the sections dealing with propagation, reflection and refraction, and dispersion of propagating waves.

TABLE 1
SUMMARY OF PROPAGATING VELOCITIES MEASURED ON NON-STRATIFIED AND STRATIFIED SOIL

Measurement Location	Instr.	Distance Between (ft)				Vel. (ft/sec)		From Fig.
		Excit. and Instr. 1	Instr. 1 and Instr. 2	Instr. 2 and Instr. 3	Instr. 3 and Instr. 4	Comp. Wave, v_c	Shear Wave, v_s	
(a) IMPACT EXCITATION, NON-STRATIFIED SOIL								
Surface	Seis.	25	25	25	—	1,100	460	5
		40	3.3	—	—	1,100	440	6
Subsurface	Press.	30	5	—	—	1,100	450	7
		33	3.3	—	—	1,100	460	8
(Average)						1,100	450	
(b) SINUSOIDAL EXCITATION, STRATIFIED SOIL								
Surface	Seis.	20	10	—	—	20 ¹	900 ²	10
		60	1.75	—	—	40 ¹	450 ²	11
Subsurface	Press.	50	3	3	3	20 ¹	300 ²	12
		60	3	3	3	30 ¹	300 ²	13

¹ Exciter frequency, in cycles per second.

² Apparent phase velocity, v_p , in feet per second.

4. It must be kept in mind that these velocities cannot be determined with greater accuracy than ± 2 percent and that the longitudinal- and transverse-horizontal components of the trajectories could not be recorded satisfactorily with the available instrumentation.

TYPE OF PROPAGATING WAVES

The purpose of the following discussion is to show that some soils, in particular sandy clays, can be classified as visco-elastic solids and approach a medium of equivoluminal characteristic (11).

Velocities

Four types of waves, two body and two surface waves, are of primary significance (Table 2).

Velocity Ratios

The ratio of the compression velocity to the shear-wave velocity yields

$$m = \sqrt{\frac{\sigma - 1}{\sigma - 1/2}} \quad (6)$$

where $m > 1.41$ and $\sigma =$ Poisson's ratio.

Poisson's Ratio

Poisson's ratio may be obtained from Eq. 6 as

$$\sigma = \frac{1/2 m^2 - 1}{m^2 - 1} \quad (7)$$

where $0 < \sigma < 0.5$ ($\sigma = 0.25$ corresponds to a perfectly elastic medium and $\sigma = 0.4$ corresponds to an almost equivoluminal medium).

Comparison of v_c and v_s with v_p

As shown in Table 1, surface measurements on non-stratified sandy clays under impact excitation at source-detector distances from 25 to 75 ft yielded average values of $v_c \sim 1,100$ ft per sec and $v_s \sim 450$ ft per sec.

Surface measurements on stratified sandy clays under sinusoidal excitation at source-detector distances of about 60 ft showed values of $v_p \sim 450$ ft per sec.

This seems to indicate that under special conditions and starting at a critical distance d_c from the exciter, a limited range exists where the velocity of the shear wave is equal to the apparent phase velocity (10, 12). This effect is discussed further in the sections dealing with synthesis, reflection, and refraction of propagating waves.

If the velocity ratio (see Table 1) is assumed to be

$$\frac{v_c}{v_s} = \frac{v_c}{v_p} \sim \frac{1,100}{450} \sim 2.45,$$

and it is further assumed that by substituting this value for m in Eq. 7 a Poisson's ratio, σ' , can be obtained:


$$\sigma' = \frac{1/2 (2.45)^2 - 1}{2.45 - 1} = 0.4.$$

This high value leads to the conclusion that loose sands to a certain extent may act similarly to an equivoluminal medium (5).

Elastic, Shear, and Bulk Moduli

Considering this quasi-equivoluminal characteristic, the determination of the moduli loses some of its physical signifi-

TABLE 2
TYPES OF WAVES

No.	Wave			Trajectory		
	Designation	Symbol	Direction of Velocity	Components	Designation	Symbol
1	Compression	C	$\rightarrow v_c$	$\leftrightarrow y$	Longitudinal	LH
2	Shear	S	$\rightarrow v_s$	$z \nearrow \downarrow x$	Transverse	TH and TV
3	Love	Q	$\rightarrow v_Q$	$z \nearrow$	Transverse	TH
4	Rayleigh	R	$\rightarrow v_R$		Long. and trans.	LH and TV

cance. However, a formal calculation might be of interest.

Elastic Modulus, E:

$$E = V_c^2 \zeta^* \frac{(1+\sigma)(1-2\sigma)}{1-\sigma} \quad (8)$$

for $\zeta = 100$ lb per cu ft, $\zeta^* = 0.00015$ lb-sec²-in.⁻⁴, $\sigma = 0.4$, $v_c = 1,100$ ft per sec, and $E = 12,200$ lb per sq in.

Shear Modulus, G:

$$G = \frac{E}{2(1+\sigma)} \quad (9)$$

Substituting the previously determined values yields $G = 4,350$ lb per sq in.

Bulk Modulus, B:

$$B = \frac{E}{3(1-2\sigma)} \quad (10)$$

Substituting the previously determined values yields $B = 20,300$ lb per sq in.

These values for E , G , and B do not deviate substantially from values obtained under static loads (11) by the triaxial shear method.

Elastic Constants (γ_1 and γ_2):

The elastic constant due to resistance in change of volume (Lamé's constant) is:

$$\gamma_1 = E \frac{\sigma}{(1+\sigma)(1-2\sigma)} \quad (11a)$$

and for $\sigma = 0.4$,

$$\gamma_1 = 1.43E \quad (11b)$$

The elastic constant due to resistance in change of shape (coefficient of rigidity) is:

$$\gamma_2 = E \frac{1}{2(1+\sigma)} \quad (12a)$$

or, for $\sigma = 0.4$,

$$\gamma_2 = 0.357E \quad (12b)$$

The rather small value for γ_2 seems to indicate that this particular soil approaches the behavior of a visco-elastic solid (7). Because of the existence of

shear waves, the designation as a fluid cannot be sustained (17).

In Figure 14 Poisson's ratio, σ , is plotted versus velocity ratios, m , and Lamé's constants, γ_1 and γ_2 .

Discussion

From these observations it may be justified to draw the following conclusion which, pending further investigations, must be restricted to non-compacted, stratified sandy clay:

1. Certain soil characteristics, such as Lamé's constants, Poisson's ratio, Young's modulus, shear modulus, and bulk modulus, as well as propagating velocities of compression and shear waves, could be determined.

2. Within a limited distance from the exciter, shear wave velocities are equal to apparent phase velocities.

3. A Poisson's ratio in the neighborhood of 0.4 leads to the assumption that this particular soil acted in some respect as an equivoluminal medium.

4. An elastic constant due to resistance in change of shape of approximately 0.36 classifies this soil as a visco-elastic solid.

5. A discrimination between shear waves, Rayleigh waves, and Q-waves, was not possible.

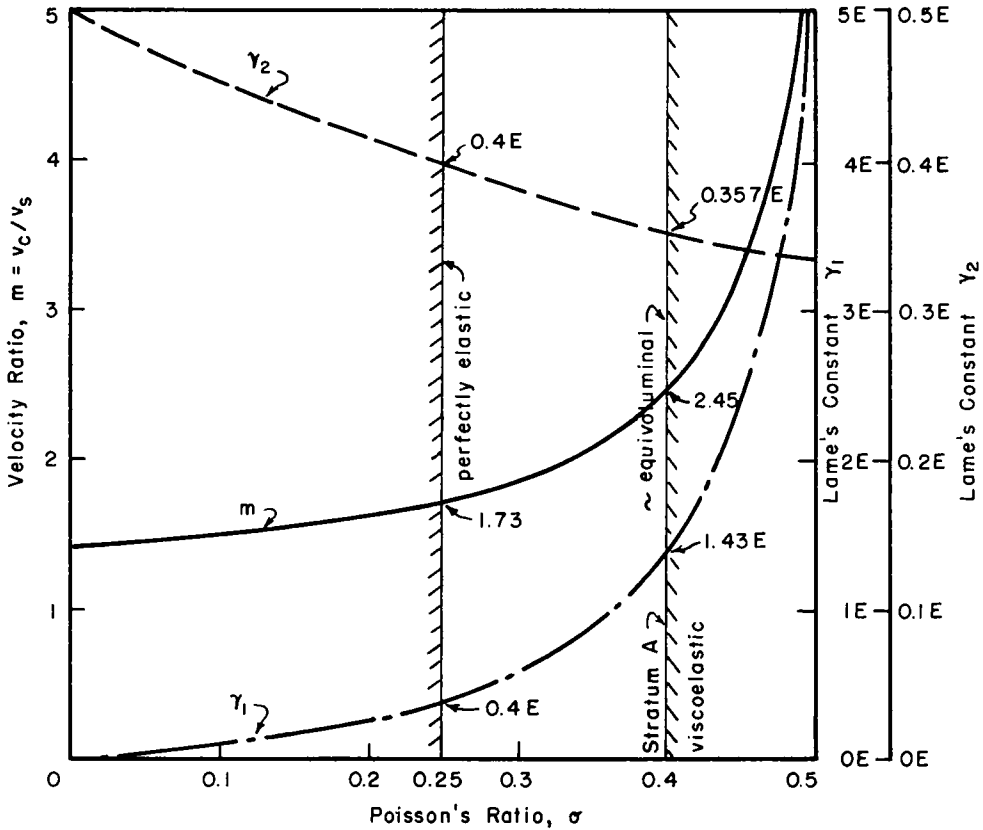
6. In this connection it should be mentioned that a number of records could not be interpreted, which might be due to some of the previously mentioned anomalies.

SYNTHESIS OF PROPAGATING WAVES

The purpose of this part of the study is to investigate whether on a stratified soil consisting of two beds with horizontal boundaries a synthesis of two decaying sinusoidal waves yields experimentally obtained distance-displacement and distance-time graphs.

The assumption is made that only two waves must be considered: one wave traveling along the surface and one wave refracted from the lower stratum.

Griggs (12) investigated a soil composed of two homogeneous, isotropic



Perfectly elastic: for $\sigma=0.25$, $\gamma_1 = \gamma_2 = 0.4E$, $m = 1.73$

Stratum A: for $\sigma=0.4$, $\gamma_1 = 1.43E$, $\gamma_2 = 0.357E$, $m = 2.45$

Figure 14. Poisson's ratio, σ , vs velocity ratio, m , and Lamé's constants, γ_1 and γ_2 .

strata. He considered three types of waves: a compression (C) wave, a shear (S) wave, and a Rayleigh (R) wave radiating from the oscillator in a sinusoidal pattern. The C- and S-waves travel through the upper bed and are reflected from the surface of the subjacent bed, the R-wave propagates along the surface.

Significant results are as follows:

1. A critical distance, d_c , exists between source and detector.

2. For distances smaller than d_c the compression wave, predominates; for distances larger than d_c the shear wave predominates (Fig. 15).

3. The value of d_c is 12.7 ft for an 11-ft deep upper stratum, and 34 ft for a 30-ft

deep upper stratum. Similar values for d_c were obtained by other methods (see "Reflection and Refraction of Propagating Waves").

4. A graph (Fig. 16) indicating the distance vs vertical displacement on the surface of a 30-ft deep upper stratum coincides reasonably well with experimental results and shows characteristic interference maxima.

General Equation

The equation for the vertical displacement amplitude of body waves can be written in the form:

$$x_b = x_a \frac{d_a}{d_b} e^{-\mu(d_b-d_a)} \quad (13)$$

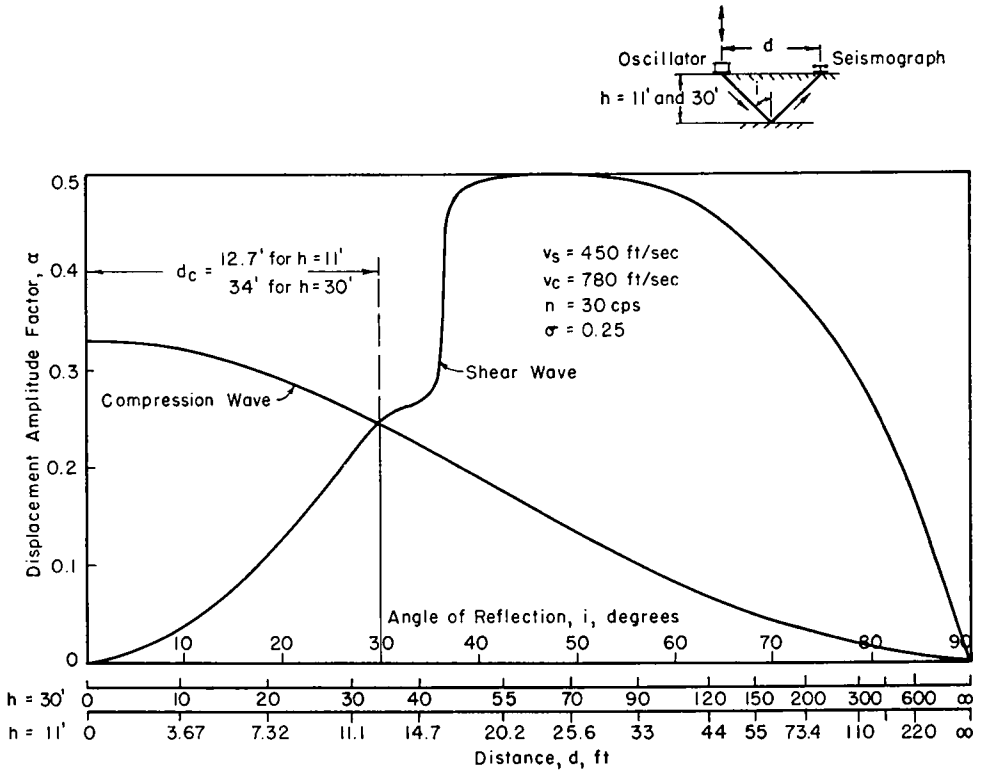


Figure 15. Displacement amplitude factors of shear and compression waves (after Griggs).

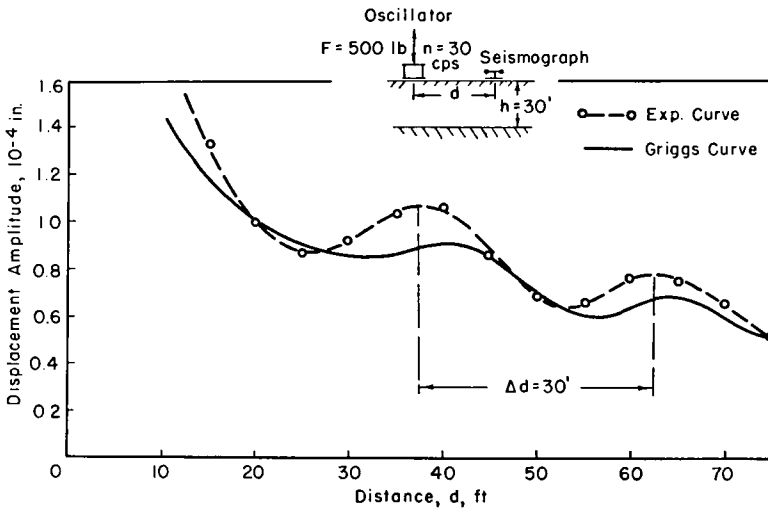


Figure 16. Distance-displacement graph, showing interference maxima.

in which

- x_a = vertical displacement amplitude at a;
- x_b = vertical displacement amplitude at b;
- d_a = source detector distance at a;
- d_b = source detector distance at b; and
- μ = decay coefficient.

But

$$\lambda = \frac{v}{n} \tag{14}$$

in which

- λ = wave length, in feet;
- v = velocity, in feet per second; and
- n = frequency, in cycles per second.

The phase angle between force and displacement amplitude has been eliminated by the experimental set-up as described in a previous report (15).

Experimental Data

In Figure 17 a set of experimentally obtained field data are plotted for a sinusoidal force vector of 500 lb with a fre-

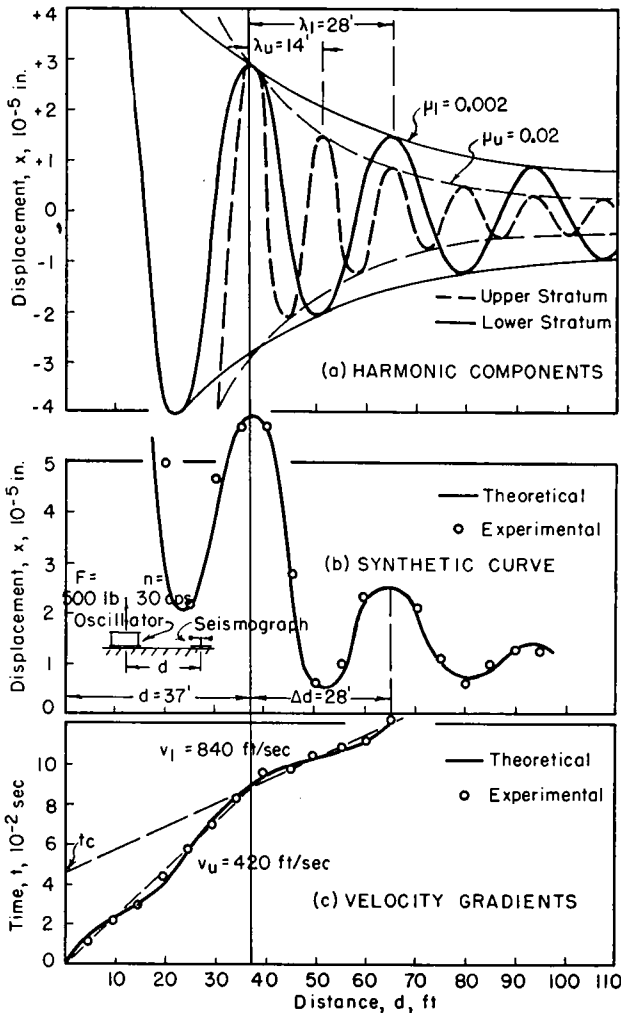


Figure 17. Determination of decay coefficient.

quency of $n = 30$ cps. Figure 17c represents the correlation between the distance from exciter to detector and the elapsed time for the propagation wave to travel the distance. Figure 17b shows this distance *versus* the vertical displacement amplitude measured by a seismometer on the soil surface. Both curves are results from experiments on strata A and B (Fig. 2).

Figure 17c yields an average phase velocity of $v_1 = 420$ ft per sec in the upper stratum and $v_2 = 840$ ft per sec in the lower stratum.

From Eq. 14, in the upper stratum $\lambda_u = \frac{420}{30} = 14$ ft, and in the lower stratum: $\lambda_l = \frac{840}{30} = 28$ ft.

The two velocity gradients intersect at the distance, $d = 37$ ft (Fig. 17c). At this distance the two vertical displacement amplitudes, x , of both waves form a maximum and are equal in magnitude and phase (Fig. 17a). For $d < 37$ ft, the velocity v_1 governs the distance-time relationship; for $d > 37$ ft, the velocity v_2 governs.

In Figure 17a are plotted two decaying sinusoidal curves representing the distance-displacement correlation of the harmonic components in the upper and lower strata. As a starting point for both waves, one-half of the experimentally obtained value for the vertical displacement amplitude, x , is selected from Figure 17b at $d = 37$ ft.

For the upper stratum (sandy clay, recent fill) a decay coefficient of $\mu_u = 0.02$, for the lower bed (consolidated sandy clay) $\mu_l = 0.002$, was assumed arbitrarily. Coefficients of similar magnitude have been reported by Heinrich (9).

Discussion

1. A synthesis of two fundamental harmonics, one traveling with the velocity of the upper stratum, the other of the lower stratum, coincides satisfactorily with experimentally obtained displacement-time and distance-time curves. Only in the vicinity of the exciter (coupling range:

$d < 20$ ft) and at greater distances ($d > 90$ ft) do larger deviations occur.

2. The gradient of the displacement-time curve represents up to the breaking point the velocity in the upper and beyond this point the velocity in the lower bed. This is discussed in more detail in the succeeding section.

3. The assumption seems justified that under certain conditions two waves predominate and that the magnitude of the selected decay coefficients for each stratum are approximately correct.

REFLECTION AND REFRACTION OF PROPAGATING WAVES

The purpose here is to check certain wave characteristics by comparing field borings with strata depth determinations from experimentally obtained distance-time, distance-displacement, and frequency-displacement graphs. The graphs are the results of surface measurements with seismographs and subsurface measurements with pressure cells.

In the following development some equations had to be expressed in the general form:

$$h_{1,2,3} = f(v_1, v_2, v_3, d, n) \quad (15)$$

where h_1 , h_2 , and h_3 represent the individual stratum depths; v_1 , v_2 and v_3 the apparent phase velocities; d the distance between source and detectors; and n the excited frequency.

Two methods of computing strata depths are discussed. The first is based on sinusoidal force excitation and follows a pattern suggested by the DEGEBO (10). The second procedure is well known from "refraction shooting" (blast excitation).

Assumptions

The assumptions made are as follows:

1. The soil within each stratum is homogeneous and isotropic and spring and damping factors are linear.
2. The reflection and refraction phenomena follow the laws of geometrical optics.
3. The interfaces acting as reflecting or refracting planes (Table 3) are consid-

TABLE 3
REFLECTING AND/OR REFRACTING PLANES (see Figure 2)

Designation	Stratum		Reflecting and/or Refracting Plane		Remarks
	Composition	Character	Between	Top of	
A	Sandy clay	Dry recent fill	A and B	B	Low density
B	Sandy clay	Dry consolidated	B and C	C	Water table height assumed to be constant
C	Sandy clay	Wet consolidated	C and D	D	
D	Clay	Hard	---	---	Moisture contents assumed to be constant High density Lens
E	Clay	Soft	C and E	E	

ered to be horizontal. These planes do not necessarily represent a change in physical composition of the subjacent strata.

4. All experiments and computations were restricted to exciter-detector distances larger than the critical distance, d_c ; that is, to the range where shear wave and reflection and refraction effects predominate.

Surface Measurements

Three typical cases are evaluated by surface measurements (see Fig. 2). These are:

Case I. — Two strata, the lower stratum of higher density than the upper stratum, or $v_1 < v_2$, corresponding to layers A and B.

Case II. — Three strata, each successive stratum with higher density than the

upper stratum, or $v_1 < v_2 < v_3$, corresponding to layers A, B/C, and D.

Case III. — Three strata, the intermediate soft stratum sandwiched between two hard strata, or $v_1 > v_2 < v_3$, corresponding to layers A/B, E, and C.

Sinusoidal Force Excitation

Figures 17c, 18a, 19a, and 20a represent experimentally obtained time-distance graphs. Figures 18b, 19b, and 20b show the arbitrarily selected ray paths for the three strata, A, B/C, and E. Figure 21 gives the corresponding frequency-displacement curves; Figures 17b and 22 give the corresponding distance-displacement curves. Numerical evaluation of these graphs for strata A, B/C, and E is summarized in Table 4.

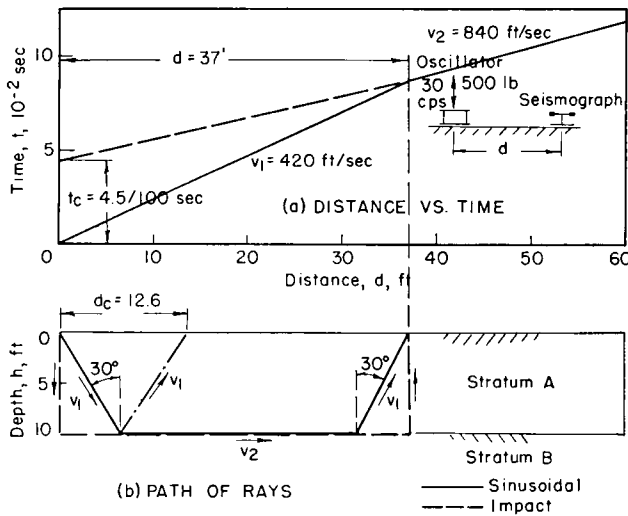


Figure 18. Distance-time graph and ray paths for surface measurements, $v_1 < v_2$.

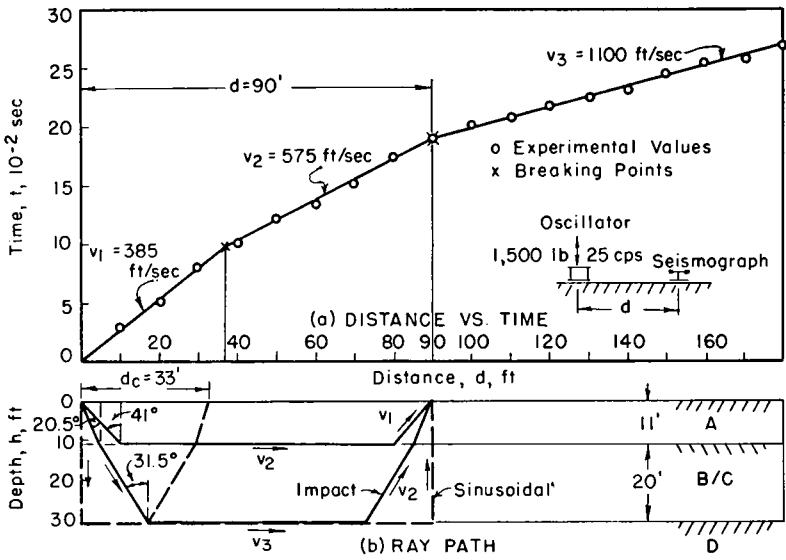


Figure 19. Distance-time graph and ray paths for surface measurements, $v_1 < v_2 < v_3$.

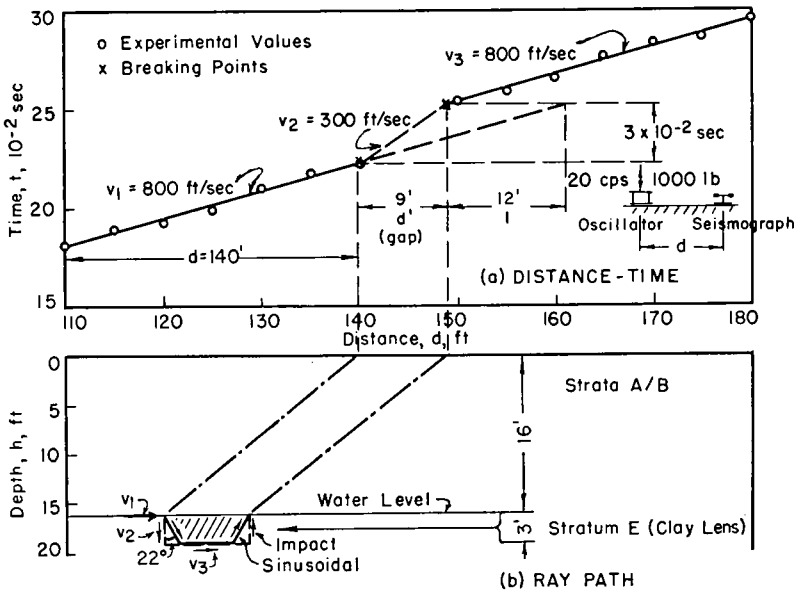


Figure 20. Distance-time graph and ray paths for surface measurements, $v_1 > v_2 < v_3$.

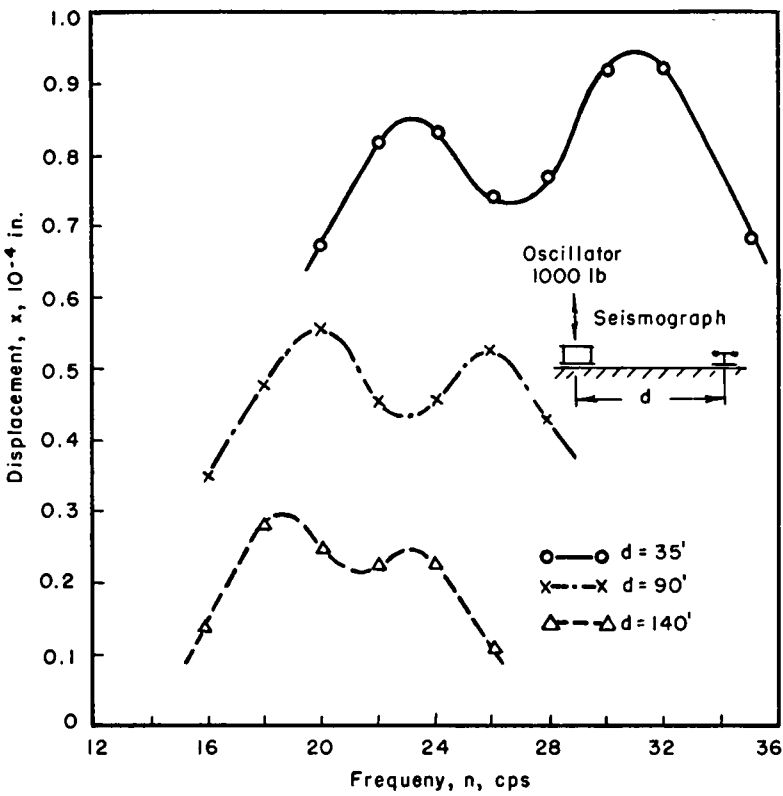


Figure 21. Frequency-displacement graph for surface measurements; determination of order number, r .

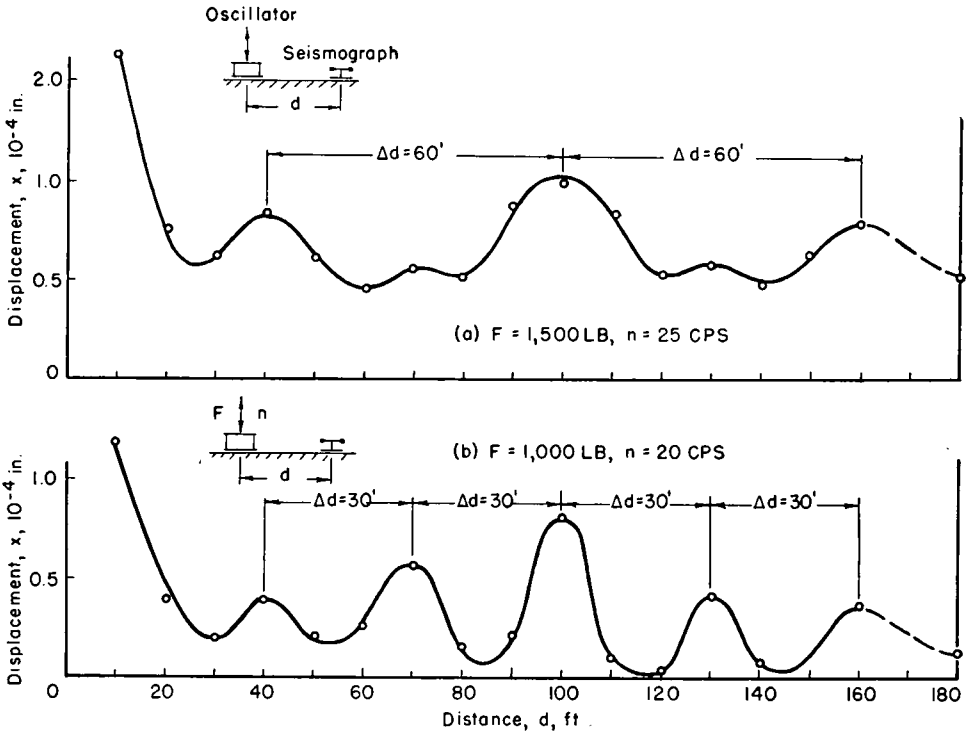


Figure 22. Distance-displacement graphs for surface measurements; determination of distance, Δd , between interference maxima.

TABLE 4
EVALUATION OF SURFACE MEASUREMENTS: SINUSOIDAL FORCE METHOD

Stratum ¹	Experimental Values					Calculated Values					λ (ft) Stratum													
	F (lb)	n ₁ (cps)	n ₂ (cps)	d (ft)	Δd (ft)	n (cps)	v ₁ (ft/sec)	v ₂ (ft/sec)	v ₃ (ft/sec)	p	r	1/nΔd (sec/ft)	1/v _n (sec/ft)	1/v _{n+1} (sec/ft)	h (ft)	r/h	Refracting Strata, Top of	A	B	B/C	C	D	E	
A	500	23 ²	31 ²	37 ³	28 ³	30 ⁴	420 ⁴	840 ⁴	—	0.74	3	0.00119	—	0.00119	0.1	11.7	B ⁸	14	25	—	—	—	—	—
B/C	1500	20 ²	26 ²	90 ⁵	60 ⁵	25 ⁶	385 ⁶	575 ⁶	1100 ⁶	0.77	3	0.00067	—	0.00083	0.12	17.8	B and D ⁶	15	—	23	—	44	—	—
E	1000	19 ²	23 ²	140 ⁵	30 ⁵	20 ⁷	800 ⁷	300 ⁷	800 ⁷	0.828	5	0.00167	—	0.00208	0.25	2.6	B and E ⁷	—	—	—	—	40	—	15

(a) CASE I—TWO STRATA— $v_1 < v_2$
 (b) CASE II—THREE STRATA— $v_1 < v_2 < v_3$
 (c) CASE III—THREE STRATA— $v_1 > v_2 < v_3$

¹ See Fig. 2. ² From Fig. 21. ³ From Fig. 17. ⁴ From Fig. 18. ⁵ From Fig. 22. ⁶ From Fig. 19. ⁷ From Fig. 20. ⁸ From Fig. 24.

Impact Force Excitation

An attempt has been made to compare the computation for sinusoidal excitation with impact excitation. The main purpose is to determine whether the different ray paths, arbitrarily selected for each method, change the results significantly. Hence, the phase velocities obtained from distance-time graphs due to sinusoidal excitation are substituted in the equation for impact excitation.

It must be kept in mind that this situation was made only for the sake of comparison and does not imply that the two types of excitation yield the same velocities at all times.

Because the case of a soft bed over a hard bed (that is, $v_1 < v_2$) is the most important one, the equation for h is represented in the form of a nomograph in Figure 23. The determination of the depth h for stratum A is indicated by Lines I, II, and III. Figures 18b, 19b, and 20b show the selected ray paths for strata A, B/C, D, and E. The evaluation for strata A, B/C, and E is summarized in Table 5.

Subsurface Measurements

Only the computation for stratum A (Case I, $v_1 < v_2$) is carried through, using again the two previously applied methods consecutively. The sensitivity of the pressure cells was too small and the disturbing forces were not strong enough to remain detectable at distances greater than 60 ft.

Figure 24a is an experimentally obtained distance-time curve; Figure 24b shows the selected ray paths. Figure 25 represents the corresponding frequency-pressure and Figure 26 the distance-pressure graph. An evaluation of these graphs for stratum A is summarized in Table 6.

A rather low velocity, $v_1 = 190$ ft per sec, observed in the upper crust from subsurface measurements is characteristic for loose sands (10). However, no explanation can be advanced as to why this velocity is lower than the corresponding velocity (420 ft per sec) gained from surface measurements.

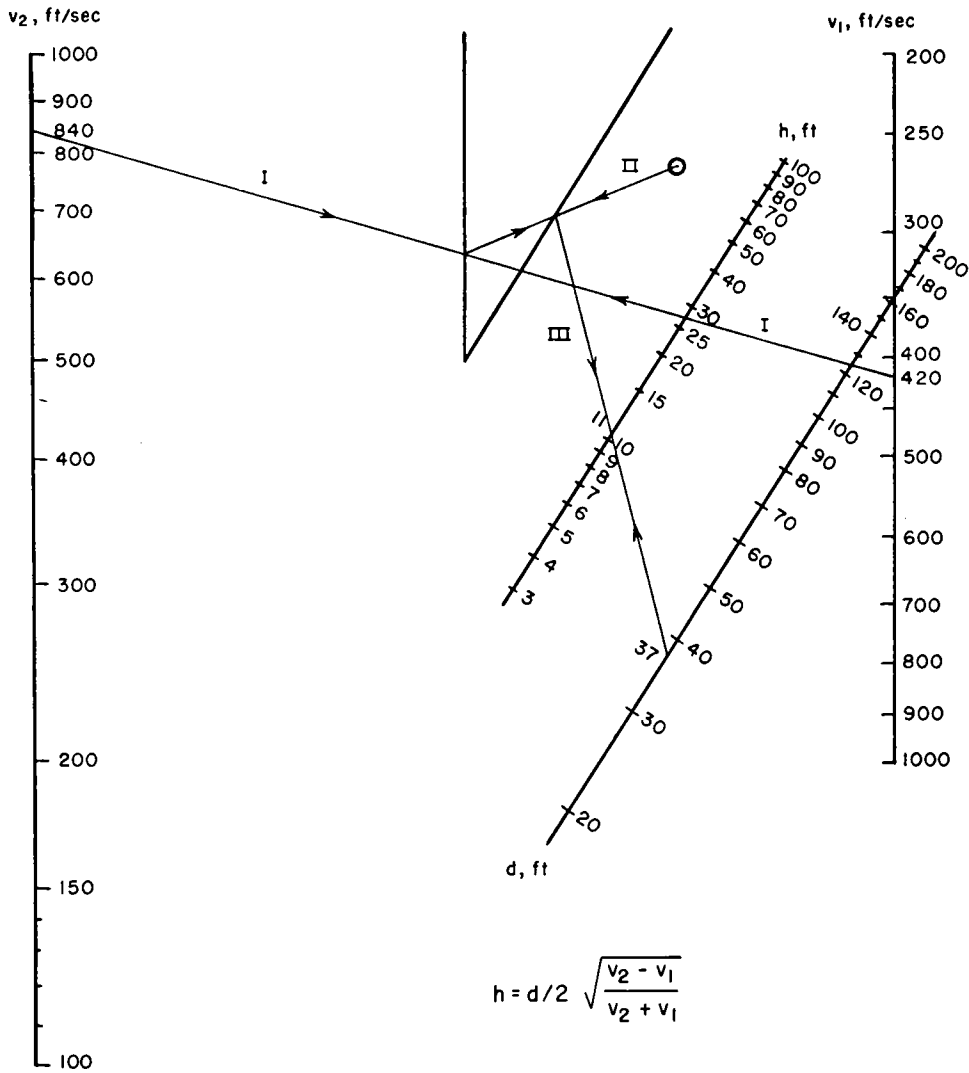


Figure 23. Nomograph for determining strata depth, h .

TABLE 5
EVALUATION OF SURFACE MEASUREMENTS: IMPACT FORCE METHOD

Stratum ¹	Experimental Values			Calculated Values						Refracting Strata, Top of
	v_1 (ft/sec)	v_2 (ft/sec)	v_3 (ft/sec)	d (ft)	t_c (sec)	i (deg)	d_c (ft)	h (ft)	h^1 (ft)	
(a) CASE I—TWO STRATA— $v_1 < v_2$										
A	420 ³	840 ³	—	37 ⁸	0.045	30	12.6	10.7	11	B
(b) CASE II—THREE STRATA— $v_1 < v_2 < v_3$										
B/C	385 ⁴	575 ⁴	1100 ⁴	90 ⁴	—	20.5—31.5, 41	33	21.3	20	B and D ⁴
(c) CASE III—THREE STRATA— $v_1 > v_2 < v_3$										
E	800 ⁵	300 ⁵	800 ⁵	140 ^{5, 6}	—	22	—	3 ²	3	B and E ⁵

¹ See Fig. 2. ² Average of maximum and minimum. ³ From Fig. 18. ⁴ From Fig. 19. ⁵ From Fig. 20.
⁶ $d' = 9$ ft, $l = 12$ ft.

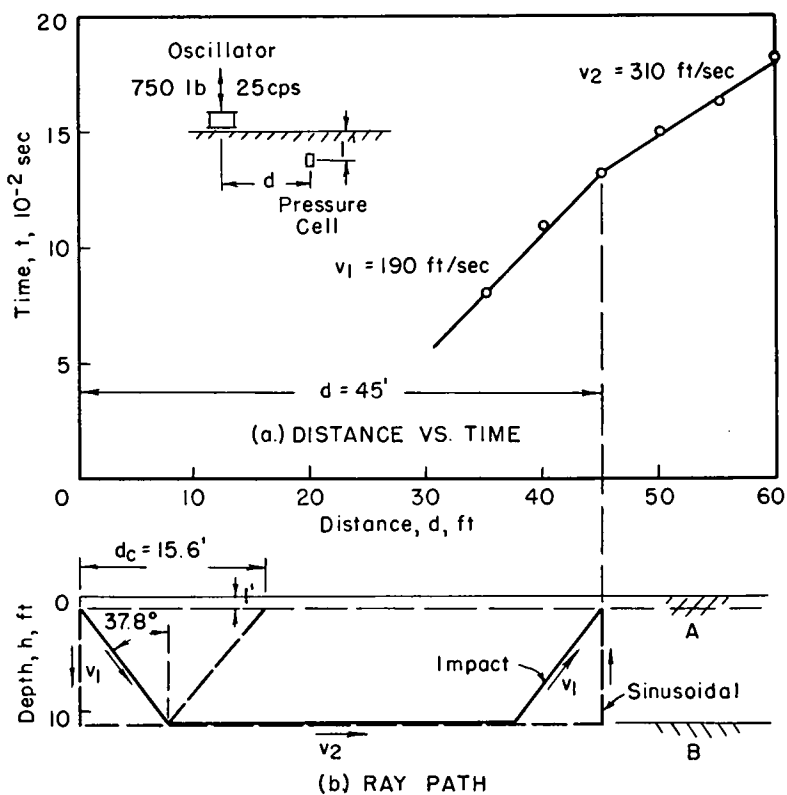


Figure 24. Distance-time graph and ray paths for subsurface measurements, $v_1 < v_2$.

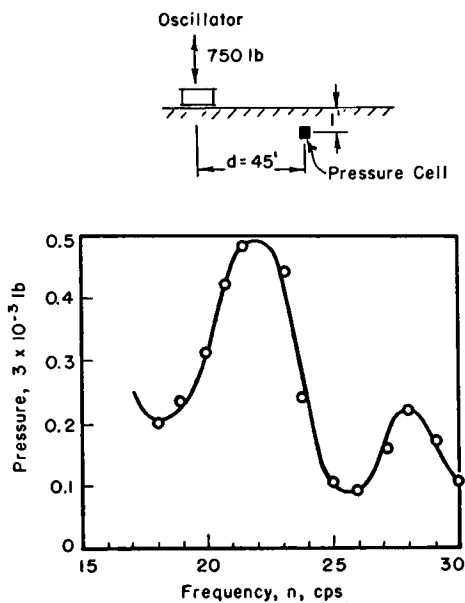


Figure 25. Frequency-pressure graph for subsurface measurements; determination of order number, r .

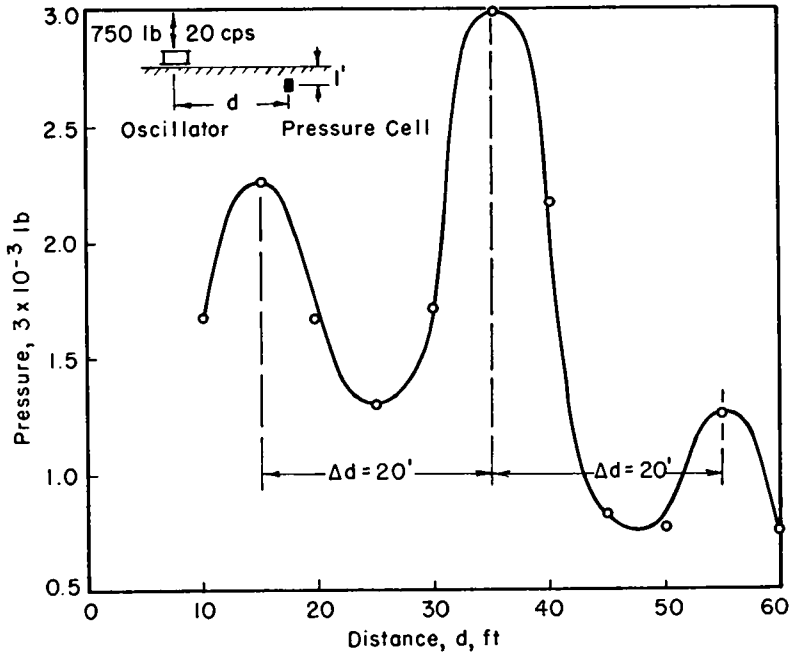


Figure 26. Distance-pressure graph for subsurface measurements; determination of distance, Δd , between interference maxima, $v_1 < v_2$.

Comparison of Sinusoidal Force and Impact Method for $v_1 < v_2$

The equation for the stratum depth, h , following the sinusoidal force method can be reduced to

$$h = \frac{v_1}{2} \frac{d}{n\Delta d} \text{ for } r = 0 \quad (16)$$

that is, for the distance d where both waves arrive simultaneously.

Substituting

$$\Delta d = \frac{1}{n} \frac{1}{1/v_1 - 1/v_2} = \frac{1}{n} \frac{v_1 v_2}{v_2 - v_1} \quad (17)$$

$$h = \frac{v_1}{2} \frac{d}{\frac{v_1 v_2}{v_2 - v_1}} = \frac{d}{2} \frac{v_1}{\frac{v_1 v_2}{v_2 - v_1}} = \frac{d}{2} \frac{v_2/v_1 - 1}{v_2/v_1} \quad (18)$$

But if

$$\frac{v_2}{v_1} = p \quad (19)$$

$$\frac{2h}{d} = \frac{p-1}{p} \quad (20)$$

An equation yielding the strata depth, h , according to the impact method, can be written in the form

$$h = \frac{d}{2} \sqrt{\frac{v_2/v_1 - 1}{v_2/v_1 + 1}} \quad (21)$$

or

$$\frac{2h}{d} = \sqrt{\frac{p-1}{p+1}} \quad (22)$$

In Figure 27 the ratio $\frac{2h}{d}$ is plotted versus the ratio, p , using Eqs. 20 and 22. From the resultant curves it follows that for both methods the maximum deviation occurs at $p \sim 1.50$ and the shape of the ray path for values $p \geq 1.50$ seems to be of minor importance. Particularly, the assumed U-shaped path, as used for the sinusoidal force method, does not alter the outcome significantly as long as the velocity ratios remain within the range investigated so far. A gradual increase in soil density with depth would modify all indirect ray pencils into smooth curves, causing the sharp breaks at the interfaces to disappear (5).

TABLE 6
EVALUATION OF SUBSURFACE MEASUREMENTS: SINUSOIDAL AND IMPACT FORCE METHODS

Stratum ¹	Experimental Values										Calculated Values					Refr. Strat., Top of	B
	v_1 (ft/sec)	v_2 (ft/sec)	n (cps)	F (lb)	n_1 (cps)	n_2 (cps)	d (ft)	Δd (ft)	p	r	$1/n\Delta d$ (sec/ft)	$1/v_2 - 1/v_1$ (sec/ft)	r/n	Sin. Force	Imp. Force		
A	190 ²	310 ²	23 ²	750 ³	228	288	45 ²	20 ⁴	0.786	4	0.002	-0.002	0.16	10.8	11		

¹ See Fig. 2.

² From Fig. 24.

³ From Fig. 25.

⁴ From Fig. 26.

Discussion

1. The arbitrarily selected shape of the ray pencils surmised in the theoretical considerations does not appear to be too critical for the studies involved, particularly for rather shallow layers.

2. The type of waves excited in both methods seems, at least for certain investigations, to be of secondary importance.

3. The supposition of one type of surface wave which is modified by another type of reflected or refracted body wave is permissible in restricted cases.

4. The rather objectionable assumption of two waves of unknown characteristics simplifies the mathematical treatment substantially; however, it should be considered as a temporary expedient only.

5. No significant qualitative contraction has been found to date between the foregoing assumptions and the experimental observations (Table 7).

DISPERSION OF PROPAGATING WAVES

The purpose here is to determine whether experimentally obtained frequency *versus* velocity graphs follow the pattern of dispersion curves plotted according to Love's theory (3, 10, 18), which is based on the propagation of Q (Quer) waves due to sinusoidal excitation.

General Equations

The Q-wave equation which contains the strata depth, h , and the velocity in the upper stratum v_1 , and the velocity in

TABLE 7
COMPARISON AND RESULTS FROM BORINGS AND MICROSEISMIC METHODS

Stratum	Type of Measurements	Stratum Thickness, h (ft)			
		Borings	Sin. Force Excitation	Impact Excitation	Love's Theory
A	Surface	11	11.7	10.7	11.5
	Subsurface	10	10.8	11	—
B/C	Surface	20	17.8	21.3	—
E	Surface	3	2.6	3.8	—

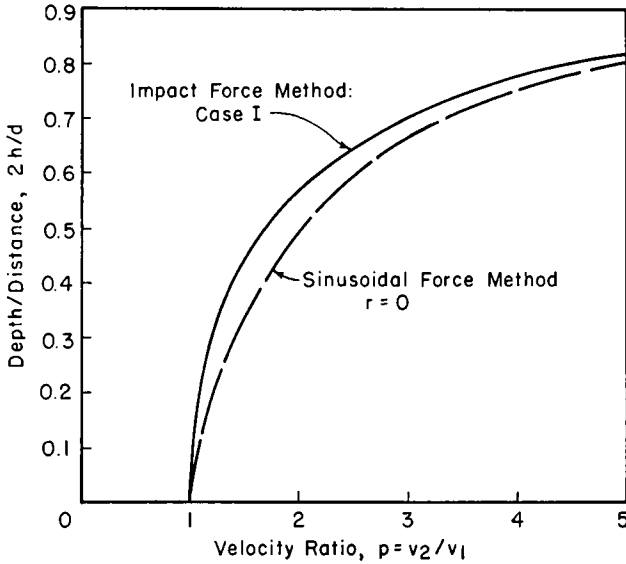


Figure 27. Comparison of sinusoidal and impact force excitation.

the lower stratum v_2 , can be written in the form:

$$\tan\left(\frac{2\pi h}{\lambda} \sqrt{\frac{v^2}{v_1^2} - 1}\right) = \frac{v_2^2}{v_1^2} \sqrt{\frac{1 - v^2/v_2^2}{v^2/v_1^2 - 1}} \quad (23a)$$

or

$$\tan(u_1 h) = \frac{u_2 v_2^2}{u_1 v_1^2} \quad (23b)$$

where

$$u_1 = \frac{2\pi n}{v} \sqrt{\frac{v^2}{v_1^2} - 1} \quad (24a)$$

and

$$u_2 = \frac{2\pi n}{v} \sqrt{1 - \frac{v^2}{v_2^2}} \quad (24b)$$

The terms for u_1 and u_2 comprise the exciter frequency n , and a velocity v , as a variable in magnitude between the limits v_1 and v_2 . The dimension of u_1 and u_2 must be $1/l$, the reciprocal of the length.

For the special case where $u_1 h = \frac{\pi}{2}$, it follows from Eq. 23a that

$$\frac{\pi}{2} = 2\pi \frac{h}{\lambda} \sqrt{\frac{v^2}{v_1^2} - 1} \quad (25a)$$

and

$$h = \frac{\lambda/4}{\sqrt{\frac{v^2}{v_1^2} - 1}} \quad (25b)$$

Let $v = \sqrt{2} v_1$, which surmises that the lower stratum is denser than the upper stratum, and $h = \lambda/4$. In other words, the maximum displacement may occur at the surface of the upper layer and a nodal plane at the boundary between both layers.

Substituting $\lambda = \frac{v}{\pi}$ in Eq. 25b yields

$$v = \frac{4nhv_1}{\sqrt{16n^2 h^2 - v_1^2}} \quad (26)$$

and v approaches infinity for the critical frequency

$$n_c = \frac{v_1}{4h} \quad (27)$$

Eq. 27 can be obtained also, starting with the well-known equation of a compressional wave in a deformable medium (slender rod):

$$n_c = \frac{v}{2l} \sqrt{\frac{E}{\zeta^*}} \quad (28)$$

where n_c = critical frequency when the induced waves in both directions combine to form standing waves; $l = \frac{\lambda}{2}$ = distance between two adjacent nodal planes; v = integers (1,2,3—); E =

Young's modulus; and ζ^* = mass density.

Let a stratum of the depth h vibrate with maximum pressure at the surface and having a nodal plane at the interface. Then $l = 2h$, $\nu = 1$ for fundamental, and $\sqrt{\frac{E}{\zeta^*}} = v_c$, or $n_c = \frac{1}{4h} v_c$, which is identical with Eq. 27. Eqs. 25b, 26, and 27 do not contain v_2 , which means that in this special case the lower stratum does not transmit any energy. Under certain conditions a standing wave will be introduced in the upper stratum and might explain the so-called "resonance" phenomena (15).

The formation of standing waves presupposes a nodal plane, but neither an abrupt nor even physical change in soil composition at a certain depth is required. For example, any variation in density or water content might facilitate the development of such a nodal plane. Hence, the often observed "natural" frequency (11, 19, 20) for any particular

vibrating oscillator-soil mass combination does not contradict the assumption of standing waves.

It is realized that Eq. 27 represents an approximate solution only, because mass, contact area and exciter force of the oscillator should be parameters of this equation.

Experimental Data

Two dispersion curves for stratum A (Fig. 2) are evaluated according to Eqs. 23a and 26.

Q waves have HT-components only, as previously shown. However, Ramspeck and Schulze (10) have shown that Eqs. 23a and 26 can be applied in modified form for waves with VT-components also. Hence, the following data are based on numerical values from experimentally obtained VT-components; that is, $v_1 = 420$ ft per sec for stratum A and $v_2 = 840$ ft per sec for stratum B (Fig. 18a).

The theoretical results have been plotted in Figure 28 and combined with ex-

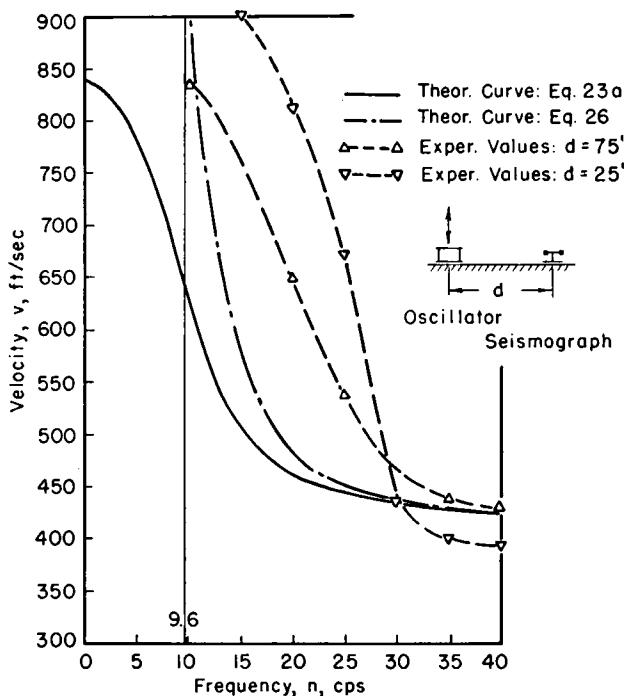


Figure 28. Dispersion curves according to Love's theory.

perimental values. The shape of the experimental curves follows, in general, Eq. 23a. However, the absolute values from Eqs. 23a and 26 differ substantially, except in the frequency range from 30 to 40 cps.

Eq. 27 yields, for $v_1 = v_c = 1,100$ ft per sec and $h = 11$ ft, $n_c = \frac{1,100}{4 \times 11} = 25$ cps.

A velocity of 1,100 ft per sec has been assumed arbitrarily. This velocity, predominating directly below the oscillator, corresponds to a compression wave for source detector distances $d < d_c$ (Table 1a). The critical frequency, n_c , coincides with independently determined natural frequencies. They were obtained experimentally from tail wave records due to impact excitation and from sinusoidal force excitation at 90° phase angle between exciter force and excited displacement amplitudes of the oscillator (15).

The following reasons might be advanced in connection with the shift of the theoretical curves to lower frequencies for $n < 30$ cps (Fig. 28):

1. The disturbing force is not a point source neither is the oscillator massless or supported by a perfectly rigid plate as surmised in the foregoing considerations.

2. For standing waves the assumption must be made that the ray pencils are grouped around an essentially vertical direction. In this case Love's equations, which are derived primarily for horizontally propagating waves with TH components, may have to be modified.

Discussion

In Table 7 are collected all results referring to strata depth determination from the sections on reflection, refraction, and dispersion of propagating waves. The height of each stratum obtained from borings is compared with the thickness derived from the previous calculations.

It must be kept in mind that borings represent limited spot checks only, whereas microseismic methods integrate over comparatively large distances (areas). As previously mentioned, the

apparent phase velocities cannot be measured with an accuracy of more than ± 2 percent. Nevertheless, the resultant deviations of h seem small enough to justify further studies under different conditions.

CONCLUSIONS

On homogeneous, stratified soils distance-time graphs can be evaluated from the arrival of wave fronts due to impact force excitation. The graphs are composed, in general, of almost straight lines with breaking points at certain distances from the disturbing source. The slopes of these lines indicate phase velocities. Close to the disturbing source phase velocities of the upper stratum, and further away the apparent phase velocities of lower strata, are presented by their gradients.

Distance-time graphs due to sinusoidal force excitation have similar forms. However, the question arises as to how these graphs can be interpreted even though no wave fronts are patterned.

For sinusoidal force excitation there has been developed by the Geophysical Institute at Göttingen in cooperation with the Technical University at Berlin (and the author's participation in the initial experiments) a method which differs from impact excitation procedures. Their most significant conclusion is that waves of shear characteristic are predominant.

A study of Griggs on propagation waves due to sinusoidal force excitation through stratified soil showed that at short distances from the disturbing force a reflected compression wave — at larger distances a reflected shear wave — becomes preponderant. This seems to indicate that under certain conditions only these wave types need be considered.

A synthesis of one surface wave and one refracted body wave, both with wave lengths corresponding to the applied exciter frequency and the measured phase velocities, yielded theoretical displacement-distance graphs similar to experimentally obtained values.

The apparent phase velocities due to

sinusoidal excitation were substituted in equations from impact excitation. The evaluated strata depths, using both methods, resulted in almost the same values which could be verified by borings (Table 7).

A theoretical dispersion curve computed according to Love's general theory is similar in shape to experimentally obtained curves (Fig. 28).

Keeping in mind that they must be restricted at present to the stratified sandy clay investigated, the foregoing results can be summarized as follows:

1. Impact excitation methods can be adapted to sinusoidal force excitation. Sinusoidal force vectors of constant amplitude independent of the exciter frequency facilitate the evaluation.

2. Certain dynamic soil characteristics could be determined by this method.

3. Special care must be taken to discriminate between reflection, refraction, and dispersion effects.

4. These phenomena might occur in case of layers with different densities and moisture contents, which do not necessarily indicate a change in physical composition of the individual soil strata.

5. To investigate upper layers, sinusoidal force excitation requires, in general, shorter wave lengths (that is, higher exciter frequencies) whereas for deeper strata longer wave lengths (or lower exciter frequencies) must be applied.

6. Further investigation is required to determine the predominant type of waves when using sinusoidal excitation.

7. A number of experimental results have been found for which no explanation can be advanced thus far. The equi-voluminal and visco-elastic behavior of the sandy clay might be the reason for some of the discrepancies.

8. Substantially more tests are required to determine the accuracy and the limitations of the methods being investigated. Of special interest would be studies to determine whether some of the dynamic soil characteristics can be correlated to the amount of consolidation, or the compaction, or the bearing capacity of any particular type of soil.

ACKNOWLEDGMENTS

This paper is an abstract of a third progress report of an investigation sponsored by the National Science Foundation. The author gratefully acknowledges the generous grants from the Foundation.

Parts of the derivations are based on previous publications as cited in the reference notes.

Most of the field tests were performed in cooperation with and on the property of the Sayreville Brick Company in New Jersey.

P. Griggs, formerly Research Assistant at the College of Engineering, Rutgers University, helped the writer during various steps of this project and analyzed a specific case under the leadership of J. J. Slade, Jr., Research Director, Bureau of Engineering Research, Rutgers University.

The continued interest of E. C. Easton, Dean of the College of Engineering, is much appreciated.

Finally, the author wishes to express his indebtedness to Professor Slade, for his valuable assistance in the preparation of the manuscript and to Professor F. J. Converse for checking the report.

REFERENCES

1. RAYLEIGH, J. W. S., "On Waves Propagated Along the Surface of an Elastic Solid." *Proc. London Math. Soc.*, Vol. 17 (1885).
2. LAMB, H., "On Propagation of Tremors over the Surface of an Elastic Solid." *Phil. Trans. Roy. Soc. London*, A, 203:1-42 (1904).
3. LOVE, A. E., "Problems of Geodynamics." Univ. Press, Cambridge, England (1911).
4. SCHLICHTER, L. B., "The Theory of the Interpretation of Seismic Travel Time Curves in Horizontal Structures." *Physics*, 3:6, 273-295 (Dec. 1932).
5. LEET, L. D., "Practical Seismology and Seismic Prospecting." Appleton, Century-Crofts, New York (1938).

- 6a. SEZAWA, K., "Propagation of Rayleigh Waves Having a Certain Azimuthal Distribution of Displacement." *Proc. Imp. Acad. (Japan)*, 4:267-270 (1928); and "Further Studies on Rayleigh Waves Having Some Azimuthal Distribution." *Bull., Earthquake Res. Inst., Tokyo Imperial Univ.*, 6:1-5 (Mar. 1929).
- 6b. SEZAWA, K., AND KANAI, K., "Decay Constants of Seismic Vibrations of a Surface Layer." *Bull., Earthquake Res. Inst., Tokyo Imperial Univ.*, 12:2, 251-257 (1935); and "Resonance Phenomena and Dissipation Waves in the Stationary Vibrations of a Semi-Infinite Body." *Ibid.*, 15:1, 1-12 (Mar. 1937); and "Resonance Phenomena and Dissipation Waves in the Stationary Vibration of the Surface of a Spherical Cavity." *Ibid.*, 15:1, 13-20 (Mar. 1937); and "On the Free Vibrations of a Stratified Body Subjected to Vertical Surface Loads." *Ibid.*, 15:2, 359-369 (June 1937); and "The Same Stationary Vibration of an Origin Accompanying Different Types of Disturbances Therefrom." *Ibid.*, 15:2, 370-375 (June 1937); and "Relation Between the Thickness of a Surface Layer and the Amplitudes of Dispersive Rayleigh Waves." *Ibid.*, 15:4, 845-859 (Dec. 1937).
7. BULLEN, K. E., "An Introduction to the Theory of Seismology." Cambridge Univ. Press (1947).
8. KELLER, G. V., "Dispersion of Seismic Waves Near a Small Explosion." *Trans. Am. Geophys. Union*, 36:6, 1035-1043 (Dec. 1955).
9. HEINRICH, A., "Über die Ausbreitung von Bodenschwingungen in Abhängigkeit von der Beschaffenheit des Baugrundes." *Die Bautechnik*, No. 51:757-761 (Nov. 30, 1930); and BIOT, M. A., "Theory of Elastic Waves in a Fluid-Saturated Porous Solid." *Jour. Acoust. Soc. Am.*, 28:2, 168-191 (Mar. 1956).
10. "Veröffentlichungen des Instituts der Deutschen Forschungsgesellschaft für Bodenmechanik (DEGEBO)." Tech. Hochschule, Berlin, No. 4 (1936), and No. 6 (1938).
11. "Symposium on Dynamic Testing of Soils." Spec. Tech. Publ. 156, Am. Soc. for Testing Mat. (1953).
12. GRIGGS, P., "Displacement of Sinusoidal Earth Waves Radiating from a Point Source." Thesis, Rutgers Univ., New Brunswick, N. J. (1956).
13. KNOPOFF, L., "Small Three-Dimensional Seismic Models." *Trans. Am. Geophys. Union*, 36:6, 1029-1034 (Dec. 1955); and "The Attenuation of Compression Waves in Lossy Media." *Bull. Seismol. Soc. Am.*, 46:1, 47-56 (Jan. 1956).
14. BERNHARD, R. K., "A Practical Application of Artificial Vibrations." *Proc. HRB*, 15:228-293 (1936).
15. BERNHARD, R. K., "On Microseismics." Spec. Tech. Publ. 206, pp. 83-102, Am. Soc. for Testing Mat. (1956).
16. BERNHARD, R. K., "Study on Mechanical Oscillators." *Proc. ASTM*, 49:1016-1036 (1949).
17. JEFFREYS, H., "On Travel Times in Seismology." *Travaux Scientifiques*, Ser. A, No. 14 (1936); and MATTICE, H. C., AND LIEBER, P., "On Attenuation of Waves Produced in Visco-Elastic Materials." *Trans. Am. Geophys. Union*, 35:4, 613-624 (Aug. 1954).
18. MACELWANE, J. B., AND SOHON, F. W., "Introduction to Theoretical Seismology." Part I, "Geodynamics." John Wiley and Sons, New York (1936).
19. CONVERSE, F. J., *et al.*, "Vibration Compaction of Sand — 1952"; "Vibration Compaction of Cohesive Soils — 1954"; and "Further Studies on Vibration Compaction of Cohesive Soils — 1955." Reports by Calif. Inst. Tech. to U. S. Navy.

20. CONVERSE, F. J., "Compaction of Cohesive Soil by Low-Frequency Vibration." *Proc. ASTM* (1956).
21. BERNHARD, R. K., "Geophysical Study of Soil Dynamics." Tech. Publ. 834; "Geophysical Prospecting," No. 55 ;and "Geophysics." *Trans. Am. Inst. Min. and Met. Eng.*, 138:326-349 (1936).
22. ISHIMOTO, M., AND IIDA, K., "Determination of Elastic Constants of Soils by Means of Vibration Methods: Modulus of Rigidity and Poisson's Ratio." *Bull.*, Earthquake Res. Inst., Tokyo Imperial Univ., 14:632-657 (1936) ; and 15:2, 67-85 (Mar. 1937).
23. NISHIMURA, G., AND TAKAYAMA, T., "The Vibration Due to Oblique Incident Waves of a Surface Stratum Adhering Closely to the Subjacent Medium and the Properties of Its Resonance Conditions." *Bull.*, Earthquake Res. Inst., Tokyo Imperial Univ., 15:2, 394-440 June (1937).
24. IIDA, K., "Determination of the Elastic Constants of Superficial Soil and Base Rock at Maru-no-uti, Tokyo." *Bull.*, Earthquake Res. Inst., Tokyo Imperial Univ., 15:3, 836 (Sept. 1937).
25. BERGSTRÖM, S. G., AND LINDERHOLM, S., "A Dynamic Method for Determining Average Elastic Properties of Surface Soil Layers." *Proc. N, R7*, pp. 1-47, Swedish Cement and Concrete Res. Inst., Royal Tech. Univ., Stockholm (1946).